Experimental and Numerical Study of Nozzle Plume Impingement on Spacecraft Surfaces

A.D. Ketsdever[1], T.C. Lilly[2], S.F. Gimelshein[2], and A.A. Alexeenko[2]

[1] *US Air Force Research Laboratory, Propulsion Directorate, Edwards AFB, CA 93524 USA*
[2] *University of Southern California, Dept. of Aerospace and Mechanical Eng. Los Angeles, CA 90089 USA*

Abstract. An experimental and numerical effort was undertaken to assess the effects of a cold gas (T_o=300K) nozzle plume impinging on a simulated spacecraft surface. The nozzle flow impingement is investigated experimentally using a nano-Newton resolution force balance and numerically using the Direct Simulation Monte Carlo (DSMC) numerical technique. The Reynolds number range investigated in this study is from 0.5 to approximately 900 using helium and nitrogen propellants. The thrust produced by the nozzle was first assessed on a force balance to provide a baseline case. Subsequently, an aluminum plate was attached to the same force balance at various angles from $0°$ (parallel to the plume flow) to $10°$. For low Reynolds number helium flow, a 16.5% decrease in thrust was measured for the plate at $0°$ relative to the free plume expansion case. For low Reynolds number nitrogen flow, the difference was found to be 12%. The thrust degradation was found to decrease at higher Reynolds numbers and larger plate angles.

INTRODUCTION

When in orbit, spacecraft require on-board or secondary propulsion systems to perform orbit transfer, orbit maintenance, and attitude control maneuvers. An important issue in the use of any spacecraft propulsion system involves the assessment and reduction of effects caused by the interaction between the thruster plume and spacecraft surfaces [1]. Direct impingement of a thruster plume on surfaces can generate unwanted torques, localized surface heating, and surface contamination. Self impingement (i.e. the impingement of a thruster plume on a host satellite surface) generally occurs for small surface angles with respect to the propulsion system's thrust vector or occurs in the thruster backflow. Cross impingement (i.e. the impingement of one spacecraft's thruster plume onto another spacecraft) can occur at essentially any angle and is becoming increasingly important with the advent of microsatellite constellations. Many studies, both nuermical [2-4] and experimental [5-6], have been performed by various investigators to assess the impingement of plumes onto surfaces.

In recent years, micropropulsion systems have been developed to address the need for highly mobile microspacecraft. A wide array of concepts will require the expansion of propellant gases through microscale nozzles. Because many micropropulsion systems will also operate at relatively low pressures, the investigation of low Reynolds number flow has become increasingly important. [7] The Reynolds number at a nozzle throat is given by

$$\mathrm{Re}^* = \frac{\rho^* a^* d_t}{\mu^*} \qquad (1)$$

An experimental and numerical effort has been developed to assess the effects of a nozzle plume impinging on a simulated spacecraft surface. The nozzle flow impingement is investigated experimentally using a nano-Newton resolution force balance and numerically using the Direct Simulation Monte Carlo (DSMC) numerical technique. The purpose of this work is to extend previous nozzle plume impingement results [5] to the low Reynolds number flow range for application to micropropulsion systems. The Reynolds number range investigated in this study is from 0.5 to approximately 900.

1. REPORT DATE **13 JUL 2005**	2. REPORT TYPE **N/A**	3. DATES COVERED **-**	
4. TITLE AND SUBTITLE **Experimental and Numerical Study of Nozzle Plume Impingement on Spacecraft Surfaces**		5a. CONTRACT NUMBER	
		5b. GRANT NUMBER	
		5c. PROGRAM ELEMENT NUMBER	
6. AUTHOR(S)		5d. PROJECT NUMBER	
		5e. TASK NUMBER	
		5f. WORK UNIT NUMBER	
7. PERFORMING ORGANIZATION NAME(S) AND ADDRESS(ES) **US Air Force Research Laboratory, Propulsion Directorate, Edwards AFB, CA 93524 USA**		8. PERFORMING ORGANIZATION REPORT NUMBER	
9. SPONSORING/MONITORING AGENCY NAME(S) AND ADDRESS(ES)		10. SPONSOR/MONITOR'S ACRONYM(S)	
		11. SPONSOR/MONITOR'S REPORT NUMBER(S)	
12. DISTRIBUTION/AVAILABILITY STATEMENT **Approved for public release, distribution unlimited**			
13. SUPPLEMENTARY NOTES **See also ADM001792, International Symposium on Rarefied Gas Dynamics (24th) Held in Monopoli (Bari), Italy on 10-16 July 2004. , The original document contains color images.**			
14. ABSTRACT			
15. SUBJECT TERMS			

16. SECURITY CLASSIFICATION OF:			17. LIMITATION OF ABSTRACT **UU**	18. NUMBER OF PAGES **6**	19a. NAME OF RESPONSIBLE PERSON
a. REPORT **unclassified**	b. ABSTRACT **unclassified**	c. THIS PAGE **unclassified**			

EXPERIMENTAL SET UP

The DeLaval nozzle used in this study had a throat diameter of d_t = 1.0 mm and an expansion ratio of ε = 62.42 and has been described in previous work. [8] The thrust produced by the nozzle configuration, in the absence of any surfaces, was measured on the nano-Newton Thrust Stand (nNTS), which has been described in detail by Jamison, et. al. [9] The nNTS was installed in Chamber-IV of the Collaborative High Altitude Flow Facility (CHAFF-IV). CHAFF-IV is a 3 m diameter by 6 m long stainless steel vacuum chamber that was pumped by a 1 m diameter diffusion pump with a pumping speed of 25,000 L/s for nitrogen and 42,000 L/s for helium. The ultimate facility pressure was approximately 10^{-6} Torr with operational pressures up to 2×10^{-4} Torr. After the free expansion thrust was measured, an electropolished aluminum engineering surface (length=width=2.54cm) was attached to the thrust stand in the configuration shown in Fig. 1. The total force measured on the nNTS for this configuration is given by

$$F_t = \Im_p - F_s + F_b \tag{2}$$

where $\Im_p$ is the thrust produced by the nozzle in the absence of the plate, F_s is the incident shear force on the plate (acting in the opposite direction as the thrust force), and F_b is the force exerted on the plenum wall due to gas pressure in the backflow. The angle α was varied from $0°$ to $10°$. The surface temperature was held constant throughout at T_S=300K.
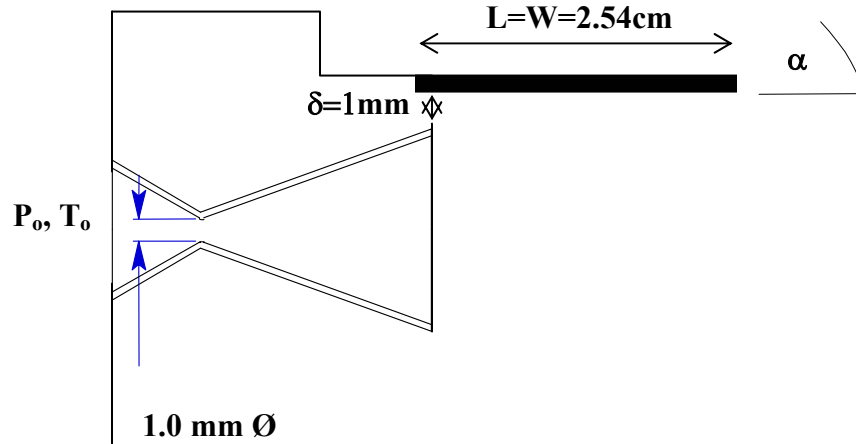

FIGURE 1. Nozzle-surface configuration.

The propellant was introduced into the nozzle plenum through an adjustable needle valve located downstream of an MKS® mass flow meter. The propellant gas temperature was held constant at T_o=300K. Nitrogen and helium were used as propellant gases in this study.

NUMERICAL METHOD

The DSMC-based software system SMILE [10] was used in all DSMC computations. The important features of SMILE that are relevant to this work are parallel capability, different collision and macroparameter grids with manual and automatic adaptations, and spatial weighting for axisymmetric flows. The majorant frequency scheme was used to calculate intermolecular interactions. The intermolecular potential was assumed to be a variable hard sphere. Energy redistribution between the rotational and translational modes was performed in accordance with the Larsen-Borgnakke model. A temperature-dependent rotational relaxation number was used. The reflection of molecules on the surface was assumed to be diffuse with complete energy and momentum accommodation.

The three-dimensional plume-surface interaction was modeled using a starting surface at the nozzle exit, generated using an axisymmetric solution (also obtained with SMILE). An elliptic distribution function was used for inflow molecules. The number of simulated molecules and cells was about 40 million and 3 million, respectively. The computational geometry included the nozzle with the external side of the plenum and the plate which size and location correspond to the experimental setup.

RESULTS

Figure 2 shows the thrust obtained in the experiments by the nNTS for a helium flow. Figure 2(A) shows a decrease in the measured thrust when the engineering surface is attached to the nozzle (as in Fig. 1) due to the shear force produced by the plume impingement. For the surface at α=0°, the thrust decrease is approximately 16.5% compared to the free expansion nozzle thrust. Larger α increases the measured thrust due to decreased plume impingement on the surface. For α=10°, the thrust degradation is only 7.0% compared to the free expansion case. Presumably, the measured thrust would approach the free expansion limit as α tends to 90°. As the Reynolds number (mass flow) increases, the difference becomes less pronounced as shown in Fig. 2(B). Figure 3 shows similar results for a nitrogen flow. In the low mass flow cases, the thrust decrease is 12.0% and 4.9% for α=0° and α=10°, respectively. Note that the thrust for the surface impingement cases begins to approach the free expansion case beginning at a mass flow of 80 SCCM for nitrogen. Figure 3(B) shows that that the thrust measured for the α=10° case is approximately equivalent to the free expansion thrust at mass flows above 200 SCCM. At higher Reynolds numbers, the nozzle plume becomes less divergent due to higher axial velocities and the reduction of the viscous interaction layer inside the nozzle geometry. Therefore, the plume impingement on the engineering surface decreases as the Reynolds number increases. It should be noted that for a given stagnation pressure, the Reynolds number for nitrogen is roughly a factor of 3 larger than helium leading to the transition to the free expansion case at lower mass flow rates for nitrogen as shown in the differences between Fig. 2(A) and Fig. 3(A).
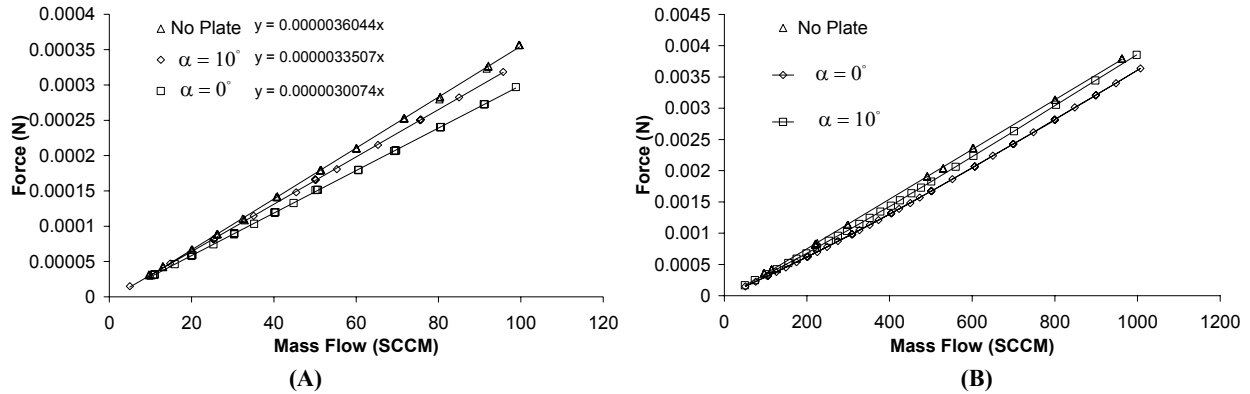

FIGURE 2. Thrust versus mass flow for helium propellant. Measurements for free expansion, and engineering surface at α=0°and 10° (A) Mass flow from 0 to 100 SCCM, (B) Mass flow from 100 to 1000 SCCM.

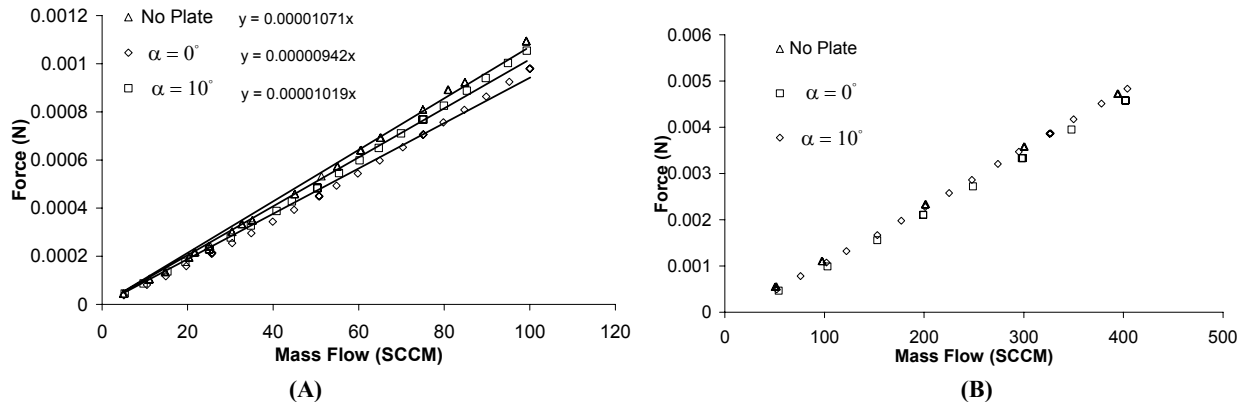**FIGURE 3.** Thrust versus mass flow for nitrogen propellant. Measurements for free expansion, and engineering surface at α=0°and 10° (A) Mass flow from 0 to 100 SCCM, (B) Mass flow from 50 to 400 SCCM.

DSMC Results

The pressure flow field, normalized by the stagnation pressure, is given in Fig. 4 for a nitrogen flow at Re=60. The interaction region between the plume and the plate is clearly seen in Fig. 4, with the local pressure maximum located near the plate surface about 7mm downstream from the nozzle exit plane. The pressure values in that region are over an order of magnitude larger than those at the corresponding location in the bottom half of the plume. There is significant backflow observed as the result of the plume-surface interaction. A strong backflow will result in a noticeable contribution of backflow molecules interacting with the plenum surface (F_b) to the total force. This contribution increases the total force in x-direction. The increase in α from 0 to $10°$ significantly weakens the plume-surface interaction, as shown in Fig. 4(B). The pressure maximum is more than two times smaller for $10°$ than it was for $0°$, and the plate no longer has a noticeable effect on the flowfield in the immediate vicinity of the nozzle exit. The backflow pressure is also reduced and is only slightly higher than the corresponding pressure at the bottom half of the plume backflow.

As mentioned earlier, the increase in the stagnation pressure causes a less divergent plume. This is illustrated in Fig. 5, where the pressure field is given for nitrogen flow at Re=270. As a result, the difference between the pressures near the surface and the corresponding undisturbed values (bottom half of the plume) is smaller than for Re=60. The local pressure maximum near the plate shifts downstream to about 12mm from the nozzle exit plane. The plume backflow formed due to the plume-surface interaction is lower than the Re=60 case. The increase in the plate angle further decreases the backflow as seen in Fig. 5(B).

The quantitative impact of the plume on the plate surface is shown in Fig. 6 where the force in axial direction (shear force) is given. The force maximum is located at about 10mm from the exit plane. The negative force at the upstream part of the plate is due to the influence of backflow molecules. The force is negative even at small axial distances, which means that the force there is governed by molecules that come from the main plume and not the boundary layer of the nozzle. These molecules come primarily from the plume scattering and those molecules reflected from the surface. The region of negative force in x-direction increases with the plate angle as shown in Fig. 6(B). The location of the maximum force is close for both $\alpha=0°$ and $10°$, whereas the magnitude of the maximum is over a factor of two lower for $\alpha=10°$. Increasing the Reynolds number shifts the maximum shear force location downstream and stretches the force isolines in the axial direction.

The contribution of the plume force ($\Im_p$), plate shear force (F_s), and the backflow force (F_b) that acts on the plenum to the total force (F_t) is given in Table 1 for nitrogen. For lower Reynolds number, the plate shear force amounts to about 20% of the plume force for $\alpha=0°$ and over 8% for $\alpha=10°$, while the backflow force is about 3% and 1.5%, respectively. These contributions are reduced almost two times for the higher Reynolds number case. The results for a helium flow are qualitatively similar to those for nitrogen. In addition, the computations were performed for a 80% diffuse and 20% specular surface using the Maxwell gas-surface interaction model. These computations showed that plate shear force and the backflow force are proportional to the percent of molecules reflected diffusely, which implies a relatively small impact of plume-surface interaction region (or, more accurately, molecules reflected from the surface), on plume molecules impinging on the surface.

Result Comparison

Figure 7 shows the comparison of the DSMC results with the experimental data for the total force (F_t) as a function of mass flow for the engineering surface at $\alpha=0°$ and $10°$. The DSMC results are within 2% of the experimental results at Re=60. The greater disagreement between the two results at Re=270 is most likely caused by the finite background pressure in the facility at the higher flow rates. As discussed by Ketsdever [11], the background gas pressure can cause a thrust degradation on the order of a few percent in the thrust range considered in this work. Similar agreement between the DSMC and experimental results has also been found for helium flows.

CONCLUSIONS

DSMC results have compared to within a few percent of experimental measurements of the total system force for a nozzle plume impinging on an engineering surface with nitrogen and helium cold gas propellants. For low Reynolds number, the plate shear force was found to be approximately 20% of the nozzle's free expansion thrust when the plate was parallel to the flow. For larger angles (α) and Reynolds number, both the surface shear force

and the backflow force on the plenum decreased. As a result, the total force measured tended towards the free expansion thrust. The DSMC results have also shown that the surface shear force and the backflow force are proportional to the percent of molecules that reflect diffusely. For the cases investigated in this study of cold gas (T_o=300K) impinging on a cold surface (T_s=300K), the momentum accommodation coefficient is near unity.
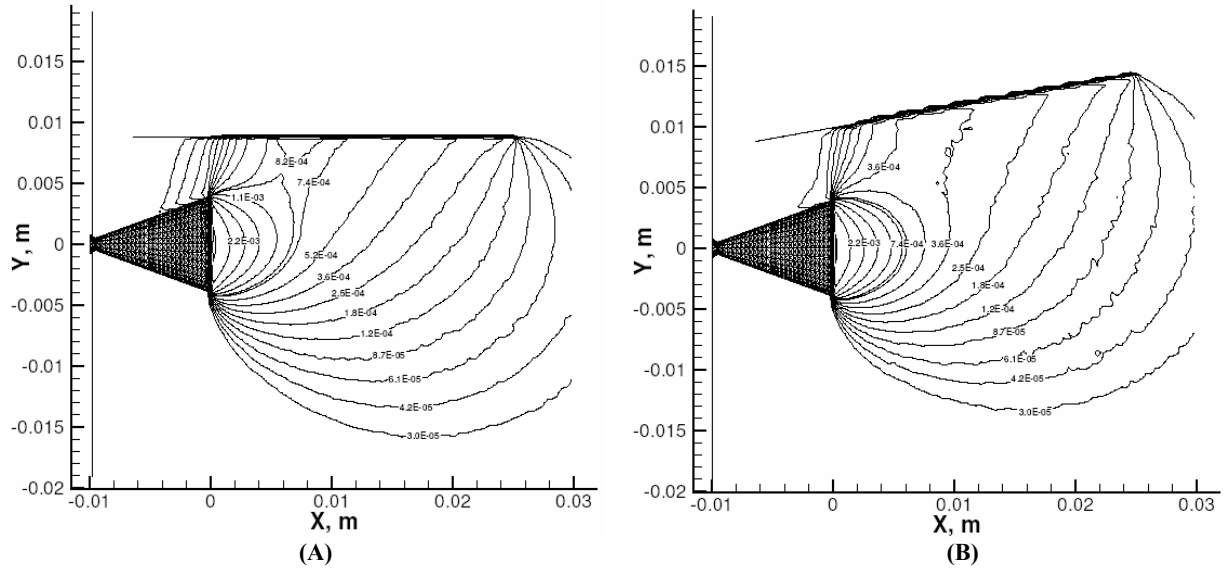

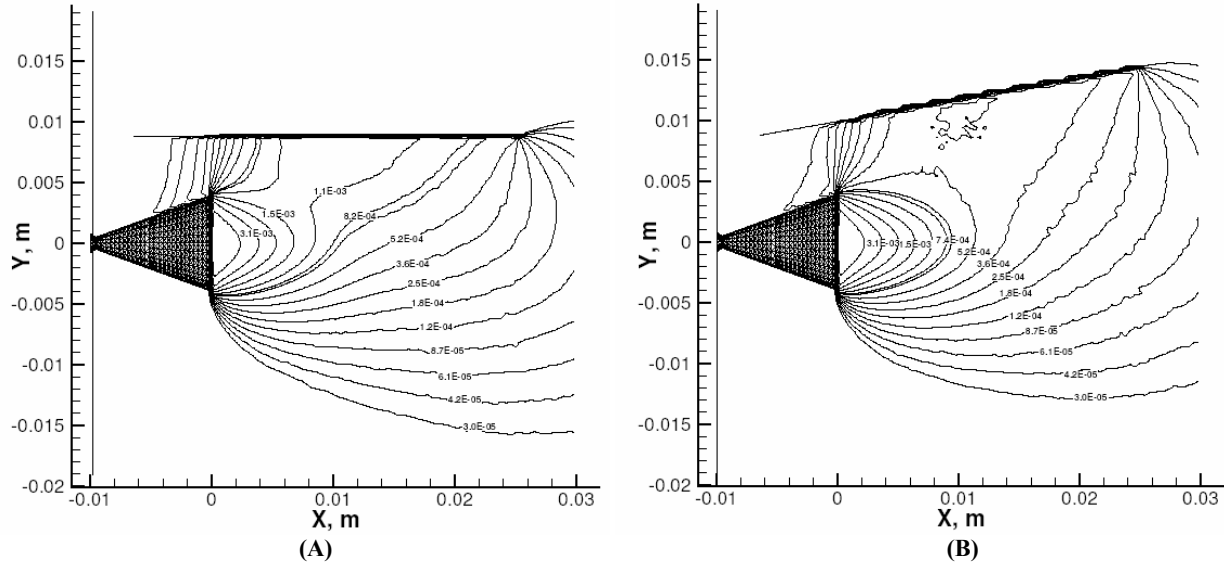**FIGURE 4.** Pressure profiles for Re=60 nitrogen flow. (A) α=0°, (B) α=10°.

FIGURE 5. Pressure profiles for Re=270 nitrogen flow. (A) α=0°, (B) α=10°.

REFERENCES

1. Boyd, I. and Ketsdever, A., J. Spacecraft and Rockets, 38, 380 (2001).
2. Lengrand, J-C., Allegre, J., Bisch, D., Skovorodko, P., "Impingement of a Simulated Rocket Exhaust Plume onto a Surface," in Rarefied Gas Dynamics – Proceedings of the 20th International Symposium, edited by C. Shen, Bejing University Press, Beijing, 1997, pp. 537-542.
3. Ivanov, M., Markelov, G., Kaskhovsky, A., Giordano, D., "Numerical Analysis of Thurster Plume Interaction Problems," in Proceedings of Second European Spacecraft Propulsion Conference, ESA SP-38, 1997, pp. 603-610.
4. Hyakutake, T., Nishida, M., "Numerical Simulation of Rarefied Nozzle Plume Impingements," in Rarefied Gas Dynamics, Proceedings of the 22nd International Symposium, edited by T. Bartel and M. Gallis, AIP Conference Proceedings 585, American Institute of Physics, New York, 2001, pp. 806-811.

5. Leege, H., "Plume Impingement Forces on Inclined Flat Plates," in Rarefied Gas Dynamics, Proceedings of the 17th International Symposium, edited by A. Beylich, VCH, Aachen, 1991, pp. 955-962.
6. Deependran, B., Sujith, R., Kurian, J., "Impingement of Low Density Freejets on a Flat Plate," in Rarefied Gas Dynamics – Proceedings of the 20th International Symposium, edited by C. Shen, Bejing University Press, Beijing, 1997, pp. 465-466.
7. Ketsdever, A., Micropropulsion for Small Spacecraft, AIAA Progress Series in Astronautics and Aeronautics, eds. Micci and Ketsdever, Vol. 187, 2000, pp. 139-166.
8. Jamison, A. and Ketsdever, A., "Low Reynolds Number Performance Comparison of an Underexpanded Orifice and a DeLaval Nozzle," in Rarefied Gas Dynamics - Proceedings of the 23nd International Symposium, edited by A. Ketsdever and E.P.Muntz, AIP Conference Proceedings 663, American Institute of Physics, New York, 2003, pp. 557-564.
9. A. Jamison, A. Ketsdever, and E.P. Muntz, Rev. Sci. Instrum., 73, 3629-3637 (2002).
10. Ivanov, M.S., Markelov, G.N., Gimelshein, S.F. "Statistical Simulation of Reactive Rarefied Flows: Numerical Approach and Applications," AIAA Paper 98-2669, 31st AIAA Thermophysics Conference, Albuquerque, NM, June 1998.
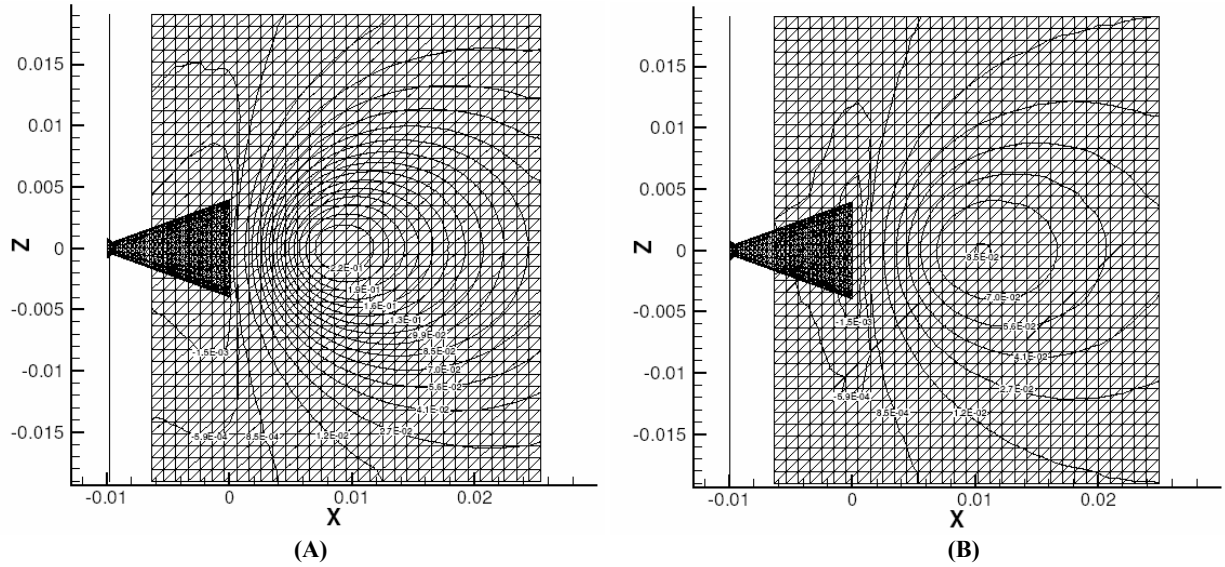11. Ketsdever, A., J. Propulsion and Power, 18, 797-804 (2002).

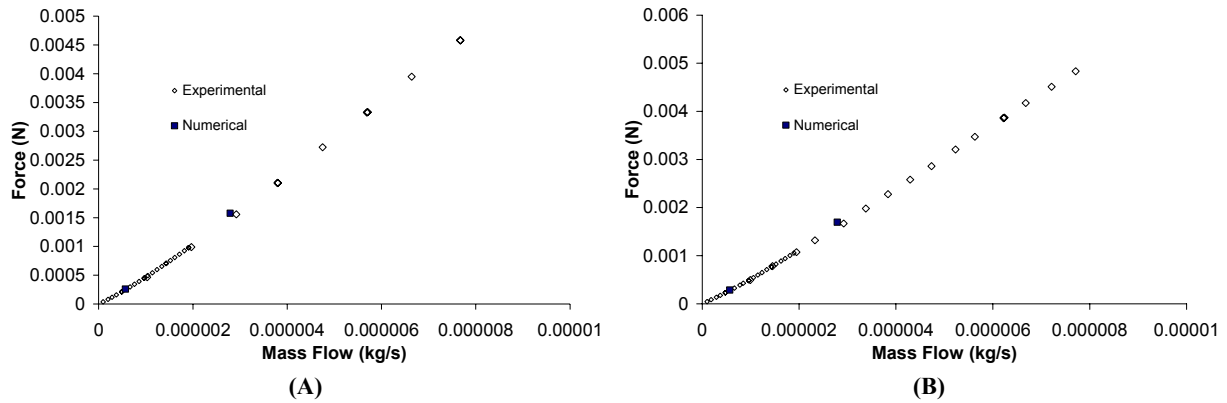**FIGURE 6.** Shear force isolines for Re=60 nitrogen flow. (A) $\alpha=0°$, (B) $\alpha=10°$.

FIGURE 7. Comparison of experimental and numerical results for nitrogen flow. (A) $\alpha=0°$, (B) $\alpha=10°$.

TABLE 1. DSMC data for nitrogen flow.

Re*	Mass Flow (kg/sec)	α (deg.)	$\Im_p$ (N)	F_s (N)	F_b (N)	F_t (N)	$F_t/\Im_p$
60	5.67E-7	0	3.076E-4	5.889E-5	1.119E-5	2.599E-4	0.845
60	5.67E-7	10	3.076E-4	2.611E-5	4.850E-6	2.863E-4	0.931
270	2.79E-6	0	1.771E-3	2.277E-4	3.414E-5	1.577E-3	0.890
270	2.79E-6	10	1.771E-3	8.906E-5	1.384E-5	1.696E-3	0.958